Variations in Terrestrial Organic Carbon Burial in Mid-Latitude Deglaciating Fjords

Victoria deJong

vdejong@uw.edu

June 5, 2026

Abstract

Carbon burial in marine sediments plays an important role in regulating global climate dynamics across glacial timescales by reorganizing the distribution of carbon across the planet. Burial of organic carbon produced by terrestrial plants is a rapid, naturally-occurring form of atmospheric carbon dioxide removal that may sequester carbon for thousands to millions of years. However, the fate of terrestrial carbon in the ocean is poorly resolved in global climate models and there remains a missing sink in the modern carbon budget. Furthermore, there remains an open question as to the role of terrestrial carbon in natural carbon dioxide fluctuations across glacial cycles. Mid-latitude fjords play a globally significant role in land-to-ocean carbon transport and burial, storing more carbon per area than other coastal and marine environments. However, the effect of rapid deglaciation on carbon sequestration in fjord sediments is not well-quantified. Here, we applied a multi-proxy approach characterizing the evolution of carbon burial in mid-latitude fjords over space and time in four sites spanning a latitudinal and off-shore gradient in the Gulf of Alaska. We interpreted glacial history and depositional environment via high-resolution sediment core CT scans and radiocarbon-based age models. We determined relative organic carbon source contribution in modern surface and aged basal sediments by analyzing bulk sediment elemental and isotopic ratios and n-alkane abundances. We found that reduced glacial presence in the drainage basin was associated with an increase in the relative percentage of terrestrial plant carbon and an overall decrease in organic carbon preservation. Understanding the mechanisms and magnitude of this natural carbon dioxide removal in these and other nearshore systems may help resolve the unbalanced modern carbon budget, distinguish natural atmospheric carbon dioxide fluctuations across glacial time from anthropogenic inputs and inform future climate change response strategies.

Plain Language Summary

The amount of carbon dioxide in the atmosphere is increasing at an unprecedented rate due to human activity. However, it also fluctuates naturally alongside changes in global temperature and ice volume as Earth cycles between ice-ages and warm interglacial climate states across millenia. Terrestrial plants harvest carbon dioxide directly from the atmosphere while organic carbon produced by marine organisms is rapidly recycled in the surface ocean and can return to the atmosphere within decades. As burial of carbon in marine sediments is one of few ways to reduce atmospheric carbon long-term, burial of land plant material may result in greater net removal than other forms of carbon. Fjords are steep, coastal environments carved by glaciers

that are highly efficient sediment burial sites. We do not know how the rapid deglaciation seen in mid-latitude fjords today will affect future carbon burial. Here we explore the amount and source of organic carbon in modern surface and aged deep sediment layers from four sites on the Alaskan margin, spanning a range of glacial extent. We found that deglaciation increases the relative amount of terrestrial plant carbon buried compared to other sources, but decreases total carbon sequestration. Understanding the relationship between glacial retreat and efficiency of long-term carbon burial offers important insights for predicting and potentially mitigating anthropogenic climate change.

Introduction

Biologically-driven, dynamic processes on the Earth's surface play a major role in regulating Earth's climate by shuffling carbon (C) between air, ocean and living organisms (Friedlingstein et al., 2025; Hedges, 1992; Zonneveld et al., 2009). Quantifying the rate and magnitude of C transfer between these rapidly cycled pools (atmosphere, hydrosphere and biosphere) and slowly cycled pools (deep-sea sediments, rocks and fossil fuels) across Earth's history is essential for distinguishing natural variations in the C cycle from anthropogenic perturbations.

Historically understudied and hence excluded from climate models, terrestrial organic carbon (tOC) input and burial in the global ocean may correspond with the "missing sink" in the global C budget (Friedlingstein et al., 2025; Hedges & Keil, 1995). Modern accounting of the global C cycle has a budget imbalance of -0.4 Gigatons of C, which implies the existence of an unknown, or underquantified, long-term C sink (Friedlingstein et al., 2025). On glacial-interglacial timescales, there remains a question as to the role tOC plays in climate systems that regulate atmospheric CO_2 changes over time. Many paleoclimate models suggest tOC is a negative feedback, releasing C to the atmosphere during cool-state glacial advances and sequestering C during warm-state glacial retreats like today (Crowley, 1995; Sigman & Boyle, 2000). However, the directionality, magnitude and timescale of C transferral is debated (Ciais et al., 2011; Jeltsch-Thömmes et al., 2019; Zeng, 2003).

Organic carbon (OC) burial is both dynamic and highly efficient in glacial fjord systems. Glacially-carved, silled fjords are steep, deep sea inlets with a shallow ridge at the mouth that constricts deep-water circulation. The resulting bottom-water low-oxygen conditions promote organic matter preservation (Hedges & Keil, 1995; Smith et al., 2015; Syvitski et al., 1987). With elevated rates of productivity and sedimentation compared to other coastal environments,

temperate fjords are estimated to contain 11-12% of the OC stored in coastal margin sediments despite having less than 0.1% of the total volume of global coastal sediments (Nuwer & Keil, 2005; Smith et al., 2015; Syvitski et al., 1987). Fjord environments are rapidly changing as glacial systems destabilize in the face of recent decades of anthropogenic warming (Black & Kurtz, 2023; Davies et al., 2024). However, the effects of ice loss and the resulting change in sediment delivery on the source and efficiency of C burial in glaciated systems remain poorly constrained across time.

Carbon provenance, or source, can be defined by the organism that originally "fixed" inorganic C from the atmosphere (primarily through photosynthesis) and incorporated it into biomass. Biogenic, or biologically-produced, tOC is "fresh" material produced by plants and is particularly understudied in marine environments. Vascular plants contain C-rich lignin and other hardy molecules that are relatively resistant to decomposition (Hedges, 1992; Hedges & Keil, 1995; Hedges & Oades, 1997). Vascular plant burial in ocean sediments may facilitate direct, rapid removal of atmospheric CO_2. However, other forms of tOC can be considered distinct from this freshly fixed C. Kerogen-rich, lithogenic tOC forms when biological matter is compressed for millennia between layers of sediment until incorporation into the bedrock. Highly recalcitrant, this ancient form of tOC is broadly inaccessible to the marine microbes that mediate rapid C cycling in the surface ocean (Hedges, 1992; Hedges & Keil, 1995; Zonneveld et al., 2009). Thus, its burial may represent the transfer of C from one long-term storage pool to another without impacting atmospheric CO_2 or global temperature. Soil, which contains a mix of eroded bedrock and degraded plant material, is another aged source of tOC (Hedges & Oades, 1997; Zonneveld et al., 2009). By contrast, marine OC (mOC) is derived almost exclusively from phytoplankton. It has a relatively homogenous composition and is rapidly remineralized in the surface ocean, capable of returning CO_2 to the atmosphere within decades (Friedlingstein et al., 2025; Hedges, 1992; Zonneveld et al., 2009). The sources and total amount of OC buried from the marine versus terrestrial pools may therefore have a strong impact on the timescales of global C cycling and distribution of C among global reservoirs in the modern climate system and through glacial time.

Distinguishing between mOC and tOC in sediments can be accomplished in several ways. In many coastal environments, the elemental ratio of organic C and nitrogen atoms (C/N) in bulk sediments reflects marine versus terrestrial origin because land plants are enriched in C—though the degree of enrichment varies vastly by species (Hedges & Oades, 1997; Maslin & Swann, 2006). The ratio of "heavy" to "light" stable C and nitrogen isotopes (δ^{13}C and δ^{15}N) is also classically indicative of OC source due to differences in fractionation during photosynthetic

C fixation and other metabolic pathways (Hedges & Oades, 1997; Maslin & Swann, 2006). Generally, the “woodier” the plant, the more C it contains and the more “light” that C is (depleted in δ^{13}C). Thus, vascular plants that predominate forests during warm interglacials like today have the highest C/N and most negative δ^{13}C while most mOC has low C/N and the least negative δ^{13}C signature. Terrestrial sources broadly contain “lighter” δ^{15}N than marine (Hedges & Oades, 1997; Zonneveld et al., 2009).

Multi-proxy analyses have proven crucial to disentangling complex elemental and isotopic signals in previous studies in the region (Kim et al., 2011a; Walinsky et al., 2009). Hydrocarbons, a class of especially large and chemically stable lipids, are useful paleoclimate proxies as they persist in sediment records longer than other forms of organic matter (Bush & McInerney, 2013; Chevalier et al., 2015; Eglinton and Hamilton, 1967). N-alkanes are straight, saturated lipid chains with varying lengths that are characteristic of the organism that produced it (Kolattukudy, 2001). As such, comparing the relative abundance of n-lengthed alkanes within sediments can indicate the relative contribution of OC sources. Primary producers of interest in fjord environments all exclusively make alkanes containing odd-numbers of C atoms: long chains (C_{27}–C_{35}) are produced by terrestrial plants, short chains (C_{15}–C_{19}) are produced predominantly by phytoplankton and mid-length chains (C_{21}–C_{25}) can be produced by submerged, marine macrophytes (such as algae and eelgrass) and freshwater plants (Bush & McInerney, 2013; Chevalier et al., 2015; Kolattukudy, 2001).

This study characterized the source and amount of OC buried in glacially-diverse fjord sediments in the Gulf of Alaska across both space and time with the goal of understanding the impact of deglaciation on C burial in the modern climate and in times of historic rapid warming. Modern sediments from the shallowest depth horizon and aged sediments from the deepest layer were analyzed to address the hypothesis that total C burial would increase with increasing glacial extent across the modern spatial gradient and back through time at the two currently deglaciated fjords due to elevated rates of glacial sedimentation while the other sites will experience no change across time. This study also addressed the hypothesis that the ratio of mOC relative to plant-produced tOC would increase with glaciation across the modern glacial gradient and back through time at currently deglaciated sites as tOC changes dominant source from fresh plant matter to lithogenic OC while the other sites will experience no change across time. This work contributes toward our understanding of the global C cycle and our ability to predict the effect of anthropogenic rapid warming on these globally important C sinks.

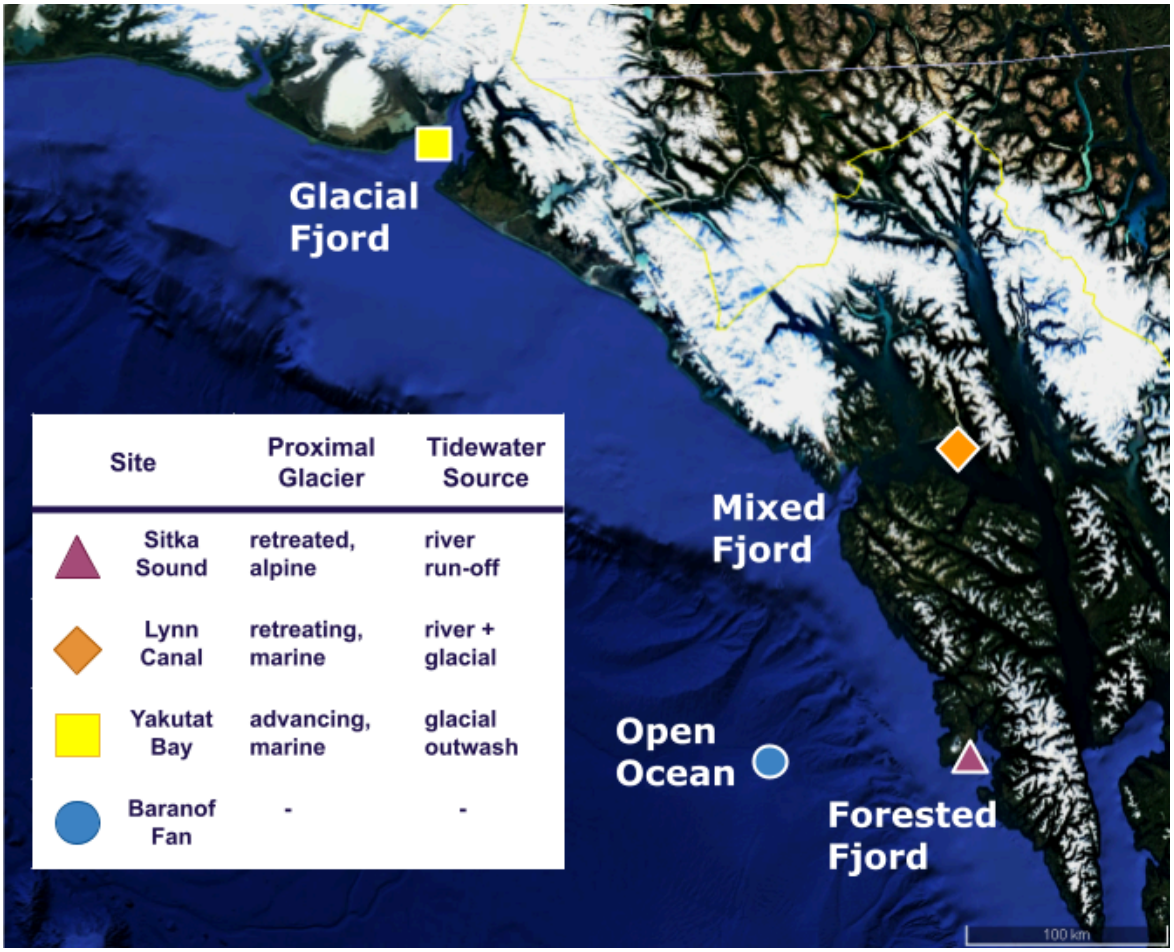

Figure 1. Map of site locations labeled with internal classification name. Legend key depicts site name, proximal glacier influence and predominant tidewater source.

Methods

Study sites

Of the four total sites, three sites span latitudinal, glacial and sediment depositional gradients along the Alaskan coast: Sitka Sound, Lynn Canal and Yakutat Bay. The fourth site on Baranof Fan was chosen to characterize an open ocean environment distant from Holocene glacial influence (Figure 1; Table 1). Although there is alpine glaciation in the drainage basin, fresh water discharge into the fully deglaciated and forested Sitka Sound is predominantly fluvial (Harris et al., 1974). Lynn Canal receives sediment from stable and retreating marine-terminating glaciers and forested river run-off (Davies et al., 2022, 2024).Yakatut Bay is fed by Hubbard Glacier, one of few rapidly advancing, marine-terminating glaciers in North America (Zurbuchen et al., 2015). Tidewater input is primarily glacial outwash, which carries

huge volumes of eroded bedrock into the inlet (Cui et al., 2016; Walinsky et al., 2009; Zurbuchen et al., 2015). The open ocean site, Baranof Fan, is on a deep-sea fan off the NE Pacific Basin continental slope that experiences hemipelagic (a mixture of predominantly lithogenic and marine biogenic) sedimentation with terrigenous contributions predominantly from the distant Alaskan and Canadian coastal ranges (Zhang & Gulick, 2020). For the purposes of this study, the locations will be referred to as Forested Fjord (Sitka Sound), Mixed Fjord (Lynn Canal), Glacial Fjord and Open Ocean (Baranof Fan) (Table 1).

Table 1. Sites including classification of proximal glacier, vegetation level, dominant tidewater source and site label.

Site Name	Cores	Latitude	Glacial Extent, Proximal Glacier	Fjord Vegetation	Tidewater Source	Site Label
Sitka Sound	19JC	57.13 N	deglaciated, alpine	forested	river run-off	Forested Fjord
Lynn Canal	16JC	58.23 N	deglaciated, marine-terminating	semi-forested	glacial, river	Mixed Fjord
Yakatut Bay	07TC, 07JC	59.93 N	glaciated, marine-terminating	non-vegetated	glacial outwash	Glacial Fjord
Baranof Fan	30TC, 30JC	56.97 N	-	-	-	Open Ocean

Core collection and characterization

Four jumbo piston cores and trigger cores were collected on cruise SKQ202410S aboard the *R/V Sikulliaq* in July 2024 (Table 1). Computer tomography (CT) scans of the sediment cores were taken at sea with Geotek Vertical X-Ray CT System (Figure 2) prior to core splitting and archival at the Oregon State University Marine Core Repository (OSU-MGR).

Sediment samples were taken at the highest and lowest available depth horizons of each core to capture the youngest and oldest sediments. The bottom two Mixed Fjord core sections were unavailable for sampling, so basal sediments and age refer to the sample depth of 1505 cm (Figure 2B). Because uppermost jumbo piston core sediments can be disturbed by the coring process, when possible we utilized trigger cores (gravity cores that sample the sediment water interface) for our surface sediment samples (Table 1).

CT scans, which are rendered from thousands of high-resolution vertical 2D snapshots of core density taken from hundreds of angles, were reconstructed with Geotek Reconstructor software to inform visual lithological interpretation. We found that some shipboard scans to be incomplete, likely due to user or instrument errors at sea. Where CT scans were unavailable,

the gap was filled in with x-radiographs, which represent average density across the entire core cross-section (as opposed to the discrete mm-scale central slice shown for the CT scan images; Figure 2A).

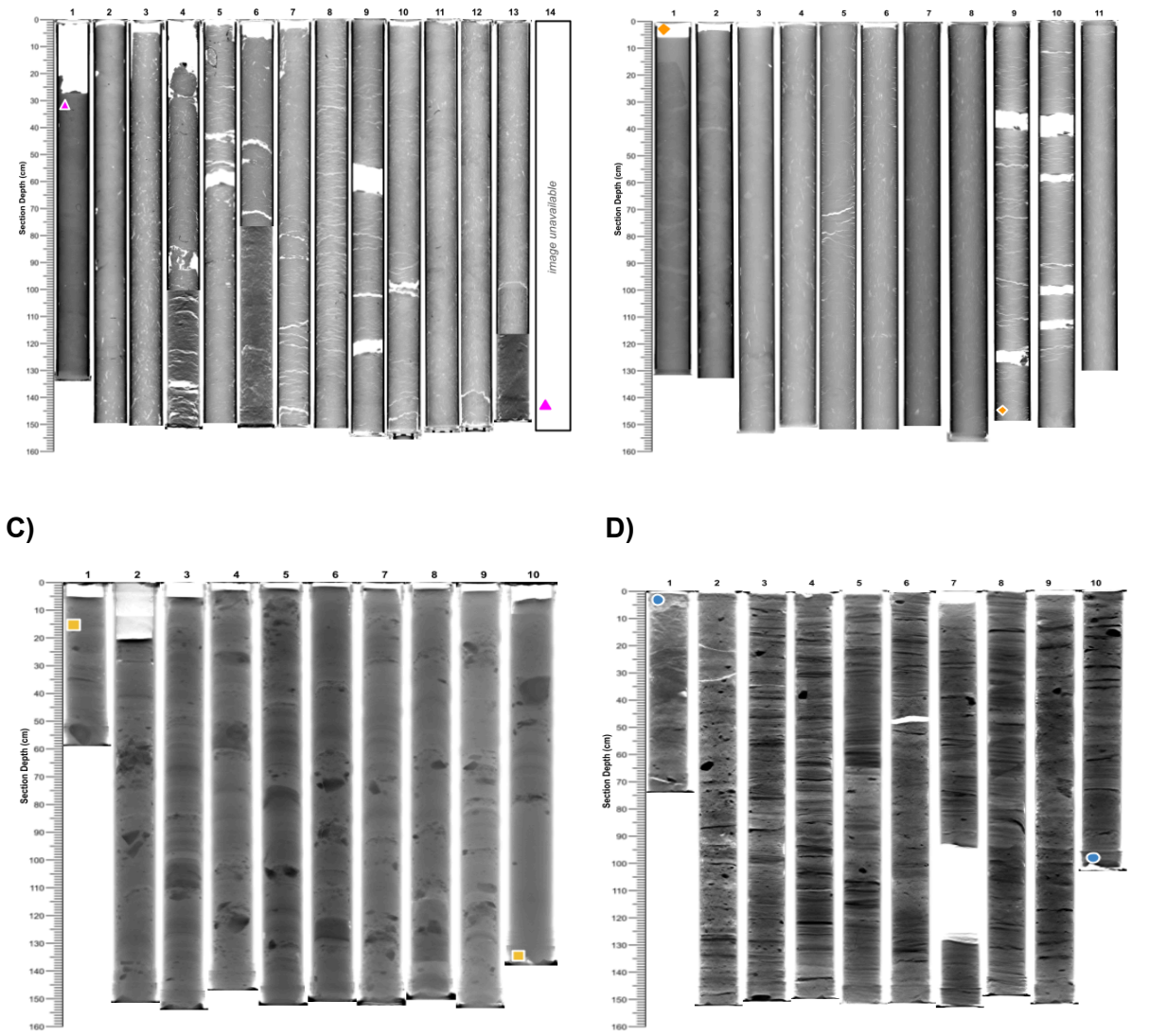

Figure 2. High-resolution CT scan reconstructions of sediment cores at each site, arranged with core sections labeled numerically increasing from left to right representing increasing down-core depth. A ruler bar depicts the relative length of each core in cm and shape markers denote sampled depths. A) Sitka Sound* (Forested Fjord) basal age 7728 +/- 203 yrs; B) Lynn Canal (Mixed Fjord) basal age 959 +/- 209 yrs; C) Yakatut Bay, (Glacial Fjord) basal age 63 yrs**; D) Baranof Fan (Open Ocean) basal age 25,350 +/- 192 yrs.

*X-radiograph images complete sections 4, 6 and 13; section 14 unavailable.
**Age estimated from layered varve counting (Ullrich et al., 2009).

Radiocarbon dating

To establish preliminary age models and calculate average sedimentation rates at each site, foraminifera fossils were sampled from the deepest horizon of each core for ^{14}C dating. To liberate foraminifera from the clay-rich sediment matrices, bulk sediment samples were first freeze-dried then wet-sieved with a 63 μm sieve and oven dried <50°C. Prior to picking for microfossils, samples were dry-sieved with 500 μm and 125 μm sieves to separate foraminifera (concentrated in the 125-500 μm fraction) from ice rafted debris (generally larger than 500 μm). Due to the highly aggregated, clay-rich matrix of certain fjord samples, some samples underwent secondary wet and dry sieving after five minutes in a low intensity sonication bath at room temperature. Fossils were picked from the dry fraction, sorted into planktic and benthic species, and etched with a mass-based calculated volume of HCl to remove the outer 10% of the shells.

All ^{14}C dates were calculated from reported raw fraction modern values (fM) using the Marine20 Calibration Curve (Heaton et al., 2020) with a marine reservoir correction of 250 +/- 100 years for planktic foraminifera based on modern water column structure (Walczak et al., 2020). For benthic foraminiferal dates, the reservoir age offset was scaled to water depth based on the D14C content of the modern Gulf of Alaska water column (Key et al., 2004). Approximate linear sediment accumulation rates were then calculated assuming surface sediments to be modern (calendar age 0). At one site (Yakutat Bay) we were unable to identify dateable material near the core base and relied on a separate, published determination of local sedimentation rates as outlined in the discussion. Burial efficiency was calculated using total OC (sample analysis described below) and linear sedimentation rate.

Bulk sediment elemental and isotopic ratios

To characterize the nature of C stored over time, bulk sediment total organic carbon (TOC) and total organic nitrogen (TON) and stable isotopic ratios ($\delta^{13}C$ and $\delta^{15}N$) were measured at the surface and base of each record. Following the vapor acidification method detailed by Hedges and Stern (1984), inorganic C was leached from ~1 g of wet sediment with 10% HCl solution and then oven dried for two days at <50°C before homogenization with a mortar and pestle. Using reported values from previous studies analyzing nearby core surface sediments (Walinsky et al., 2009) to estimate anticipated TOC and TON, sample weights were calculated using the UC Davis site calculator (Horn, 2021) before packing into silver capsules and wrapping in tin capsules. The UC Davis Stable Isotope Lab performed elemental analysis isotope ratio mass spectrometry (EA-IRMS) to produce TOC, TON, $\delta^{13}C$ and $\delta^{15}N$. C/N was

calculated by TOC/TON. Stable isotope values are reported in standard delta notation (‰) with respect to VPDB standard for C and AIR standard for nitrogen. Reported values and errors represent the average and standard deviation of two duplicate samples.

To evaluate the dominant source of C stored in sample sediments, we applied a three endmember mixing model tuned by regional measurements of coastal Gulf of Alaska terrestrial material. The “degraded” terrestrial sources include soil and Alaskan bedrock (Walinsky et al., 2009) which exhibited distinct elemental and isotopic signatures from “fresh” vascular plant debris (VPD) (Nuwer & Keil, 2005). Phytoplankton biomass fell within classically defined ranges (Hedges & Oades, 1997; Maslin & Swann, 2006; Nuwer & Keil, 2005). We defined the following C/N endmember ranges: marine = 7–10, degraded terrestrial = 10–12 and fresh terrestrial = 20–300. Considering the disproportionately large range of fresh terrestrial material, we plotted N/C which preserves the linear relationship between marine and terrestrial endmembers. This enables visual approximation of relative percent contribution using a mixing line. Marine δ^{13}C and δ^{15}N range from -20 to -22 ‰ and 5 to 8 ‰, respectively. Terrestrial endmember δ^{15}N fell between 0 to 1 ‰, while soil and regional bedrock δ^{13}C signatures were distinct from VPD (-25.5 to -26.5 ‰ and -25 to -27 ‰).

n-Alkane abundance

To contextualize the elemental data, n-alkanes were isolated from surface and basal bulk sediment samples and counted using column and gas chromatography following methods described by (Meyers et al., 1980). Samples were first oven dried <50 °C for two days before homogenization with a mortar and pestle. Total lipid extraction was performed using EDGE Solvent Extraction System using a 9:1 solution of DCM:MeOH, yielding 60mL of total lipid extract over four 90 second cycles at 100 °C. Solvents were evaporated from the total lipid extraction using N_2 gas and the n-alkanes were isolated via elution in hexane through a silica gel column (mesh size 150A). To standardize the volume of the resulting n-alkane fraction for quantitative analysis, the solvent was again evaporated and replaced with 500 uL hexane. n-Alkane relative abundance was measured using flame ionization detection gas chromatography with an Agilent GC-FID under temperatures increasing from 45 °C to 320 °C over 65 minutes. Compounds were identified and quantified by comparison to an external standard mixture (C_8–C_{28} n-alkanes) at a concentration of 10 ng/μL.

To quantitatively assess C provenance, the abundance-weighted average chain length (ACL) and terrestrial to aquatic ratio (TAR) were calculated based on relative abundance of target relevant n-alkanes. As such, biomolecules containing odd-n C atoms between C_{15} and C_{35}

were considered exclusively for ACL with values >25 representing more terrestrial contribution and <20 indicating more marine (Bush & McInerney, 2013; Chevalier et al., 2015). TAR is the ratio of common odd-n long C chains over odd-n short C chains: $C_{27} + C_{29} + C_{31} / C_{15} + C_{17} + C_{19}$ (Chevalier et al., 2015). We used the following general scale for assessing TAR: <1 dominated by aquatic organisms with strong phytoplankton productivity (highly marine), 1–5 transitional environments (mixed terrestrial and marine), 5–10 increasing dominance terrestrial plant wax over aquatic plants and phytoplankton, and >10 very strong terrestrial plant input.

Results

Site lithology and depositional history

Bioturbation, or the vertical mixing of sediment by organisms post deposition, was present throughout the entirety of the Forested Fjord (Sitka Sound) record, as evident by the lack of clear depositional layers and smooth homogenous density in the CT-scan imagery (Figure 2A). Fractures in the sediment matrix beginning ~250 cm deep indicate high gas content characteristic of post-depositional organic matter decomposition. Physical observations of the samples during ^{14}C processing indicated the sediment matrix was extremely clay-rich, brown and highly aggregated, interspersed with discrete woody vascular debris and interwoven sinewy organic material. Benthic foraminifera in basal sediments indicated sediment age 7,728 +/- 203 years, yielding a linear sedimentation rate of 266 cm/kyr (Table 2).

The Mixed Fjord (Lynn Canal) also appears bioturbated in the uppermost sediments. However, some sub-laminated primary depositional structures appear preserved vis a vis faint banding identifiable within the homogenous density upper regions (Figure 2B). Below ~400 cm, gas fractures indicate high organic content. Physical observations indicated broad similarity to the Forested sediments with limited terrestrial macrofossils and many diatom tests interwoven into the sinewy mat of organic material. The youngest datable record, basal benthic foraminifera and echinoderm spines yielded an average calendar age of 959 +/- 209 years (Table 2). The sedimentation rate was 5x greater than that of the Forested Fjord at 1570 cm/kyr.

The CT scan from the Glacial Fjord site (Yakutat Bay) captured glacial-proximal diamict characterized by a fine-grained matrix with large ice-raged clasts throughout (Figure 2C). In contrast to the other fjords, depositional structures of alternating high and low density layers suggest sedimentation rates outpace bioturbators throughout the record. Terrestrial and marine fossils were absent amid the poorly sorted, grey lithic sediment despite processing 6x the volume of sediment as the fjord samples. Other researchers have also been unable to date this

site using traditional methods including ^{210}Pb and ^{14}C (Cui et al., 2016; Walinsky et al., 2009). Ullrich et al. (2009) estimated a linear sediment rate of ~22,000 cm/kyr for a nearby core by counting presumed annual varves characterized by alternating high and low density bands of cm scale in thickness. If accurate for this environment, these sedimentation rates would imply the base of the Glacial core at 1048 cm depth is less than a century old.

The Open Ocean core (Baranof Fan) has intermittent drop stones from regional ice rafting throughout the core below ~70 cm. Uppermost sediments are bioturbated with limited preservation of primary depositional structures above ~200 cm (Figure 2D). We infer that physical laminations below 200 cm reflect depositional rates that outpace the ability of marine bioturbators to destroy physical structures such as is common in shelf fan systems nourished by expanded glacial systems (Jaeger & Nittrouer, 2006). Physical observations of the basal sediment matrix indicate a poorly sorted, unaggregated, grey, clay-rich matrix with no apparent terrestrial organic fossils. The ^{14}C basal age (from planktonic foraminifera) is 25,350 +/- 192 yrs (Table 2), near the local expression of Glacial Maximum (Cosma & Hendy, 2008). Under the constant sedimentation rate assumption used for the fjord sites, the linear sedimentation rate averages 55 cm/kyr across the entirety of the record.

Table 2. Radiocarbon dating, sedimentation rate and organic carbon burial rate by site.

Site, Sample	Sedimentation Rate (cm/kyr)	%TOC (g C/g sed)	OC Burial Rate (g C*cm/ g sed/yr)	Age (yr)
Sitka Sound	262			
Surface		7.11 ± 0.10	186	0
Base		2.46 ± 0.01	64	7728 ± 203
Lynn Canal	1569			
Surface		2.56 ± 0.01	402	0
Base		1.97 ± 0.02	309	959 ± 209
Yakatut Bay	22000			
Surface		0.32 ± 0.00	706	0
Base		0.46 ± 0.01	1015	<100
Baranof Fan	55			
Surface	14	0.95 ± 0.02	1	0
Base	110	0.32 ± 0.00	4	25350 ± 192

Note: Surface samples are assumed to be modern and basal ages were calculated with ^{14}C dating except in Yakatut Bay, which was estimated from Ullrich et al. (2009). The Baranof Fan had an independent assessment of age (~14,600 yrs at 200 cm core depth) using lithological interpretation of core CT scans corroborated with regional glacial history records (Cosma & Hendy, 2008; Davies et al., 2011).

Carbon burial efficiency

The percent of TOC in the bulk sediment (%TOC, g OC per g dry sediment) in the Open Ocean and Glacial Fjord ranged from 0.32 to 0.95 %TOC. The modern Open Ocean 2-3x more enriched than the aged sediments from the same core and both Glacial Fjord samples (Table 2; Figure 3). Aged Open Ocean and modern Glacial Fjord sediments both had 0.32 %TOC (Figure 3A). There was a higher %TOC and a larger range in the two deglaciated sites, with the Forested Fjord having the highest (7.11 ± 0.10) and lowest %TOC in total and in range, at the surface and base of the core, respectively. Modern Mixed Fjord sediments were comparable to aged Forested Fjord sediments (2.56 ± 0.01 and 2.46 ± 0.01, respectively) and modestly higher than its own basal sediments. The Forested Fjord and Open Ocean sites displayed the highest percent change from modern values, with ~65% decrease in %TOC at depth.

Table 3. Elemental and stable isotopic analysis results by site.

Site, Sample	C/N	δ13C	δ15N
Sitka Sound			
Surface	9.1 ± 0.2	-21.8 ± 0.4	7.4 ± 0.0
Base	10.0 ± 0.0	-22.3 ± 0.2	7.8 ± 0.3
Lynn Canal			
Surface	8.1 ± 0.0	-21.4 ± 0.1	6.4 ± 0.1
Base	8.5 ± 0.3	-21.2 ± 0.2	6.1 ± 0.0
Yakatut Bay			
Surface	10.7 ± 0.7	-23.9 ± 0.0	3.2 ± 0.3
Base	12.0 ± 0.1	-24.8 ± 0.0	3.1 ± 0.1
Baranof Fan			
Surface	8.1 ± 0.0	-22.5 ± 0.3	7.1 ± 0.1
Base	8.8 ± 0.5	-23.7 ± 0.0	4.1 ± 0.3

Carbon source: bulk sediment elemental and isotopic ratios

C/N also varied by site and depth, with all sites displaying modest increases in ratios with depth (C/N % change ranging from +12% at Glacial Fjord to +6% at Mixed Fjord). The Glacial Fjord had the highest C/N (11–12) and the Mixed Fjord and Open Ocean sites had the lowest (8–9) (Table 3; Figure 3B). δ^{13}C was much less variable across time and space, with the glacially dynamic Mixed and Forested Fjords least depleted in δ^{13}C (depth averaged -21 ‰ and -22 ‰, respectively) and with a smaller percent change through time (both sites experiencing <2% absolute change across depths) (Figure 3D). Glacial Fjord was the most depleted across

the record (depth averaged -23.5 with +4% change at depth). Open Ocean was slightly less depleted with a 5% percent change at depth, yielding a depth averaged -23 ‰. The depth averaged δ^{15}N across fjord sites displayed a latitudinal trend, with Forested Fjord experiencing the highest δ^{15}N enrichment and Glacial Fjord the least (+7 and +3 ‰ respectively) with modest absolute percent change between at depth (5% change) (Figure 3C). Open Ocean experienced the highest rate of change, decreasing modern enrichment from +7 to +4 ‰ at depth.

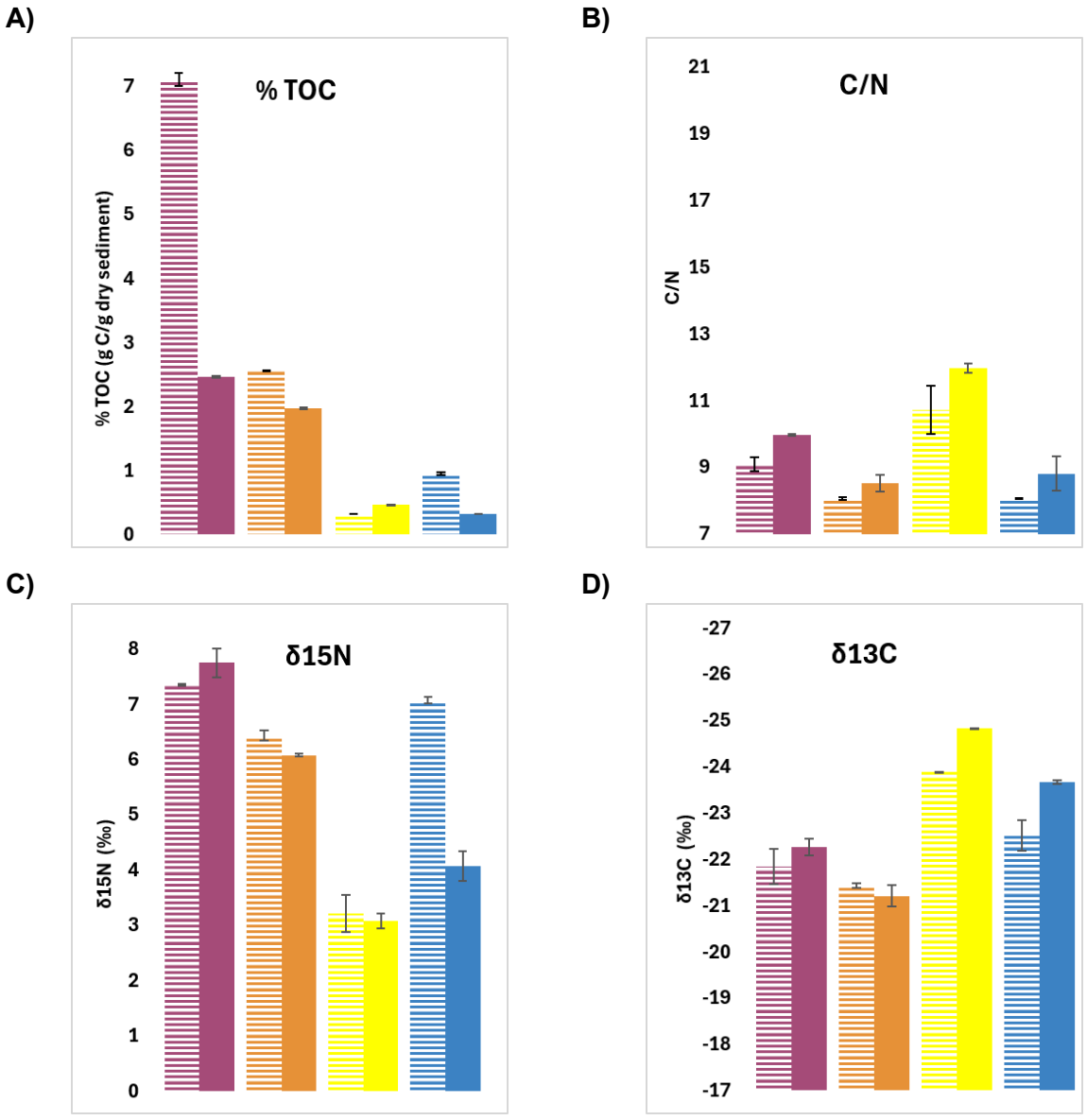

Figure 3. Elemental and stable isotope results with values representing averages and standard deviation of duplicate samples: A) %TOC in g OC per g dry sediment; B) C/N ratio; C) δ^{15}N; D) δ^{13}C. Striped represents surface sediments, solid color blocks represents basal sediments at each site, listed in the following order from left to right: Forested Fjord (mauve), Mixed Fjord (orange), Glacial Fjord (yellow) and Open Ocean (blue).

Carbon source: n-alkane abundance

The n-alkane abundances within surface and basal sediments in Forested Fjord both displayed left-skewed distributions peaking at C_{29} (877 and 327 ng/g dry sediment, respectively) and lowest abundances at C_{15} (4 and 6 ng/g dry sediment) (Figure 4A). C_{21} disrupted this skewed trend spiking as high as 416 and 66 ng/g dry sediment. Quantitative metrics indicate extremely high terrestrial input at both depths. ACL values suggested nearly identically high rates of terrestrial plant input in modern and aged sediments (27 and 28) while TAR decreased from 26 at surface to 20 at depth (Figure 5).

Modern Mixed Fjord sediments displayed a similar left-skewed distribution of n-alkanes peaking at 340 ng/g dry sediment at C_{29} and anomalously spiking at 125 ng/g dry sediment at C_{21} (Figure 4B). Basal sediments, contrastingly, had a “flattened peak” with similarly high abundances across C_{27}–C_{29} with C_{27} slightly elevated at 223 ng/g dry sediment. ACL values across depths match Forested Fjord while TAR suggests slightly less terrestrial input (11 at the surface, 17 at depth) (Figure 5).

The Glacial Fjord distribution of n-alkanes is less skewed and steep with highest concentrations at C_{27} measuring 106 and 206 ng/g dry sediment at surface and at depth with a slightly elevated spike at C_{19} (Figure 4C). ACL and TAR are consistent across depths (24 and 1, respectively) and indicate elevated marine productivity (Figure 5).

Open Ocean sediments had a lower overall abundance of n-alkanes than any fjord samples. Surface sediments followed a left skewed distribution with maximum abundance at C_{29}, 88 ng/g dry sediment (Figure 4D). Modern ACL matched the glacially dynamic sites while TAR was moderate at 10. Aged sediments appeared decidedly more marine with ACL and TAR calculating to 23 and 1, respectively (Figure 5). The maximum abundance of identifiable n-alkanes in the basal sediments was 36 ng/g dry sediment, however the chromatogram also displayed high concentrations of unchromatographically-resolvable organic matter (UCM) with a high “basement” abundance of unidentifiable biomolecules and many indistinguishable peaks preventing the identification of compounds greater than C_{27}. UCM is characteristic of unidentifiable thermogenically altered biomaterial, which can be produced by diagenesis or metamorphism during the creation of sedimentary rocks (Wang et al., 2014). As such, ACL and TAR may give values suggesting artificially low terrestrial input.

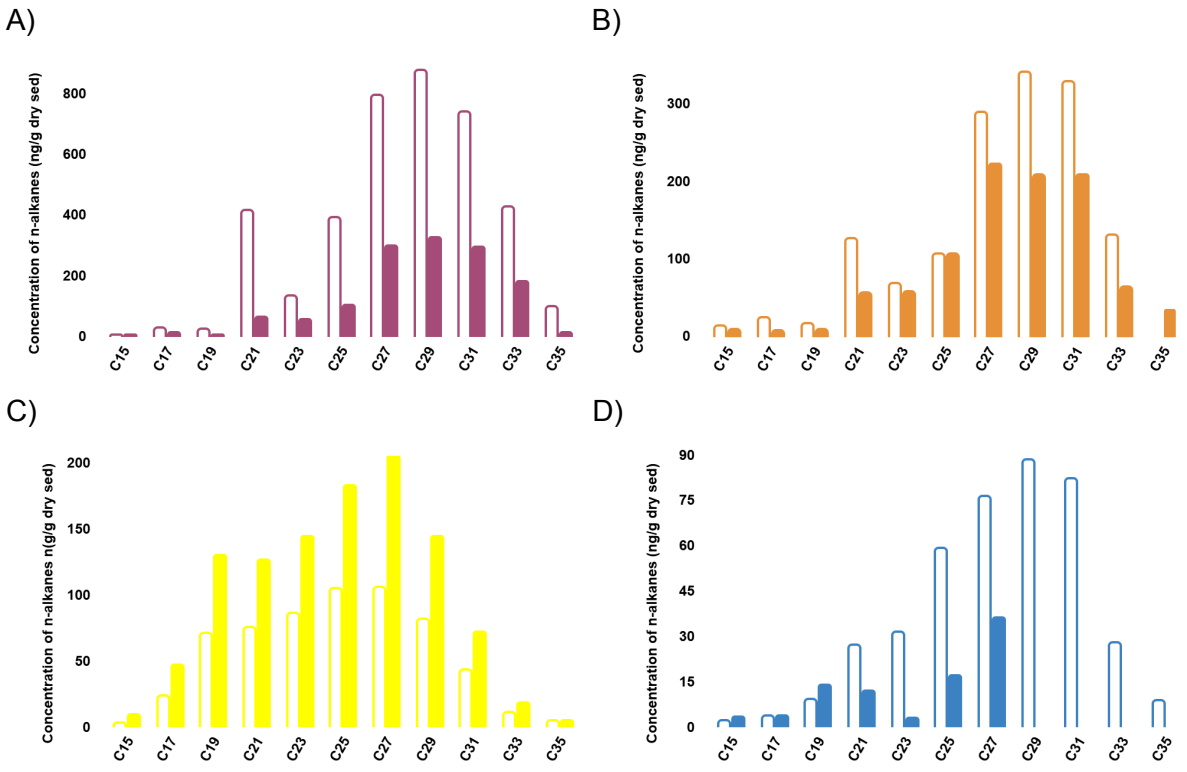

Figure 4. Distributions of n-alkane concentrations in ng/g dry sediment by site: A) Forested Fjord (mauve); B) Mixed Fjord (orange); C) Glacial Fjord (yellow); D) Open Ocean (blue). Surface sediments are depicted with hollow bars, basal with solid color bars.

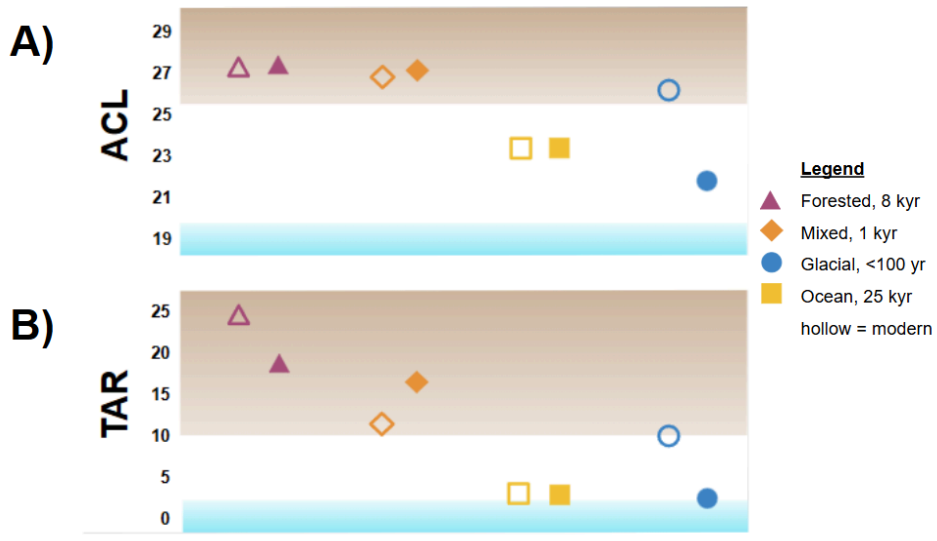

Figure 5. n-Alkane calculated metrics are plotted with endmember ranges denoted using shaded box regions for mOC (aquamarine blue) and tOC (brown). Open shapes denote surface samples and solid shapes basal samples from each site. A) Weighted-average chain length (ACL) of n-alkanes (ACL) and B) terrestrial-to-aquatic ratio (TAR).

Discussion

Glacial sedimentation increases carbon burial efficiency

The four study sites reflect a breadth of depositional lithologies and accumulation rates that parallel the presence and behavior of the glacial ice supplying terrigenous sediments to each environment. The jumbo piston cores recovered from all three margin sites recovered exclusively Holocene sediments (Table 2), dating well after the Cordilleran ice sheet retreated back to the modern coastline (Davies et al., 2011). The clear, northward increase in sediment accumulation in modern fjord sediments aligns with other experimental, observational and modeled evidence of the dominant role of temperate glaciation in determining sediment supply to margin systems (Jaeger & Koppes, 2016).

Surprisingly, the Open Ocean was the only site to display depositional evidence of glacial dynamism, as evidenced in the distinct shift from characteristic glacial sequences to bioturbated layers interspersed with drop stones ~200 cm depth (Figure 2D). Similar to observations of Pleistocene deposition on the Alaskan Surveyor Fan, the laminated sedimentary lithofacies in the lower section of the core were likely produced by turbidity currents spreading across the Baranof Fan, supplied by hyperpycnal turbid flows discharged from the shelf-crossing ice sheets (Jaeger et al., 2014). The bioturbated sediments peppered with ice rafted debris likely record the subsequent shoreward travel of the Baranof ice stream sediment depocenter accompanying rapid ice sheet retreat. The cessation of ice rafted debris above ~70 cm is interpreted to represent the conclusion of large-scale ice sheet retreat. Further to the north on the Kayak Slope, well-dated deglacial records suggest this retreat into the modern coastline occurred ~14,700 years ago (Davies et al., 2011). This timing is corroborated by a 50kyr continuous record southward which correlates a rapid drop in sedimentation from 400 cm/kyr to 53 cm/kyr ~14,600 years ago due to rapid warming and retreat of Cordilleran sheet (Cosma & Hendy, 2008). We leverage this stark depositional transition to allow an independent assessment of core age and infer lowered sedimentation rates in 1-2 m of the core and substantially elevated below. Assuming that 200 cm in the core is ~14,600 years ago, late glacial sedimentation is likely ~110 cm/kyr, while Holocene sedimentation is ~15 cm/kyr.

We interpret the depositional homogeneity within the fjord cores to represent relatively stable environmental conditions that preclude temporal down-core analysis. As such, we reserve interpretation to the modern spatial question. We can thus consider a new useful grouping of the samples the directionality of proximal glacial behavior: those recording glacial retreat or deglaciation (aged and modern Forested and Mixed fjords and modern Open Ocean)

and those recording glacial advance or active glaciation (aged and modern Glacial Fjord and aged Open Ocean).

The awesome increase in sedimentation associated with glacial advance appears to outweigh the accompanying decrease in %TOC as the rate of OC burial increases with glacial extent across the modern fjord system and in the Open Ocean site through time (Table 2). Thus, C appears to be buried more efficiently with increased ice extent, suggesting increased deglaciation from rising global temperatures will decrease total C buried in sediments in the future.

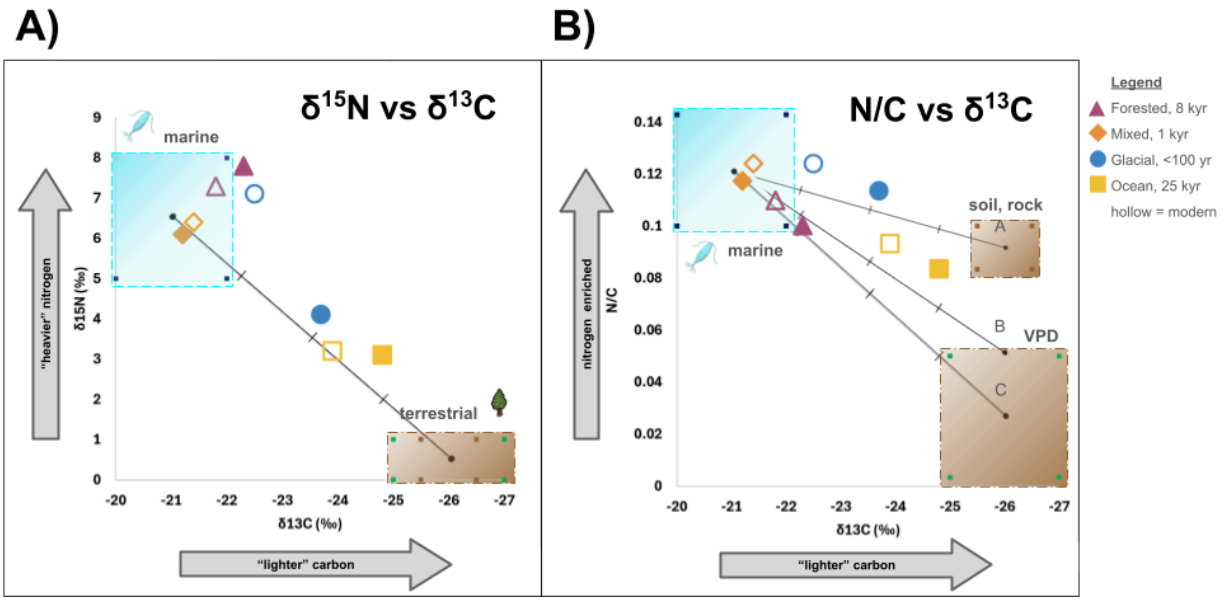

Figure 6. Endmember mixing model plots with endmember ranges denoted using shaded box regions with dashed lines (marine, aquamarine blue) and dot dash lines (terrestrial with sub-categories labeled, brown). Relative source contribution is determined by distance between each end with 25% increments marked with the middle notch denoting 50% marine, 50% terrestrial input. A) δ^{15}N vs δ^{13}C with a singular mixing line. B) N/C vs δ^{13}C with three mixing lines representing possible dominant terrestrial source regimes: a) “degraded” = soil, bedrock; b) “blended”; c) “fresh” = vascular plant debris.

Terrestrial plant burial increases in deglacial environments

The elemental and isotopic bulk sediment data suggests a broad relationship of terrestrial input with high glacial activity. All glacially-retreating sites appear majority marine while glacial advance is associated with higher terrestrial contributions (Figure 6). There is not a clear trend in OC source contribution across the modern latitudinal gradient as the Mixed Fjord

appears to be the most marine. The Forested Fjord does experience a notable decrease in marine signature in aged sediments when considering the C/N data while the Mixed Fjord appears stable over time. The Open Ocean site experiences a dramatic drop in marine signature in the Last Glacial Maximum (LGM) sample, which aligns with the aforementioned glacial sedimentation trends.

However, the n-alkane data appears to paint an inverse picture. ACL indicates terrestrial plant waxes highly dominate algal produced hydrocarbons at all glacially retreating sites while glacial advance appears to be of mixed contribution (Figure 5). TAR data indicates strong marine signals in the three samples experiencing glacial advance, while the deglaciated sites appear strongly terrestrial (10+). Plant-produced long-chain biomolecules are decreasingly evident in increasingly glacially delivered sediments across both the modern latitudinal gradient and across time in the Open Ocean record. All samples peak in the terrestrial range (C_{27}–C_{29}) which we interpreted to confirm terrestrial input is present in all samples, with highest relative abundance in those the bulk sediment ratios indicated to be most marine.

Considering the motivation of this study to analyze changes in terrestrial plant burial, specifically, we interpret n-alkane abundance to be a more robust proxy than bulk sediment elemental and isotopic ratios for terrestrial biogenic OC in these dynamic Gulf of Alaska fjord systems.n-Alkane abundances are counts of discrete, large molecules with high-energy bonds that are difficult to break down and have been demonstrated to persist in sediment records longer than other forms of organic matter. Absolute counts of plant wax biomolecules allow a more compelling argument for the presence of plant material in the sediment record than relative measurements of elemental species that can be affected by a number of metabolic processes in the water column or post-deposition.

Other studies in fjord environments found similar seemingly contradictory results between elemental data and biomarker abundance (Kim et al., 2011b; Walinsky et al., 2009). Microbially-mediated degradation has been implicated as a process distorting bulk sediment OC source signals (Zonneveld et al., 2009). Nuwer & Keil (2005) illustrated the drastic down-fjord, “microbial masking” of large, fresh plant material which appeared increasingly elementally and isotopically marine-like with distance from fjord head to sill. Furthermore, a similar transformation of tOC during oxidative exposure was demonstrated in a controlled laboratory experiment (Goranov et al., 2025). Thus, physical differences between fjords and coring sites may influence bulk sediment element and isotope signatures drastically by altering tOC transport time, complicating cross-fjord source comparisons. Lynn Canal is longer and deeper than Sitka Sound (Figure 1) and receives tidewater input from a wider variety of terrestrial

sources rather than a single glacier (like highly glacial Yakatut Bay) or solely rivers (like the forested Sitka Sound) so each fjord likely has varying tOC transport and degradation histories not directly related to proximal ice extent.

Our bulk sediment endmember mixing model may indirectly support the notion of preferential degradation of VPD within fjord systems. To apply appropriate endmember mixing models given the large C/N range differences between terrestrial sources, we inferred a dominant terrestrial source regime for each sample based on the depositional record and age model. Three regimes were considered: “degraded” (soil and/or bedrock), “blended” and “fresh” (majority vascular plants debris, VPD), denoted with mixing lines A, B and C, respectively. (Figure 6B). Deglaciated samples were attributed to a blended terrestrial source (due to the presence of vegetation and soil, with varying degrees of delivery of eroded bedrock by glaciers) and sites with active glacial advance to a degraded terrestrial source (assumed to be devoid of vegetation). Notably, increasing the presumed contribution of VPD changed the relative source to appear slightly more marine in all samples except the Mixed Fjord. If this rapid transformation does occur during transport, then increasing input of fresh plant material in deglacial systems would result in the appearance of more mOC preserved in the sediments.

Though biomarkers are less easily transformed due to chemically stable high energy bonds, even numbered n-alkanes can be produced from larger odd-numbered n-alkanes by bacterial reworking (Chevalier et al., 2015; Wang et al., 2014). All samples contained even-numbered n-alkanes, however, we excluded this from ACL and TAR calculations to constrain the data to the primary producers that initially create biomass. While this may also indicate possible bacterial influence, we recommend a targeted analysis to resolve the apparent disagreement between carbon source proxies in this mid-latitude fjord system.

Conclusion

Glaciers are powerful agents of erosion and sediment transport. Therefore, understanding their impact on the rapid sequestration of atmospheric CO_2 through the burial of terrestrial plant material is prescient to understanding past, present and future climate change. Our data suggests that active glaciation increases organic carbon burial efficiency, but decreases the amount of land plant burial relative to other sources. Contrary to expectations, the deep sea sediments on the Baranof Fan recorded dramatic glacial retreat across 25 kyrs, allowing temporal analyses to support qualitative spatial trends across the comparatively short and glacially stable fjord records. The remarkable near absence of identifiable terrestrial plant

wax remains in the LGM fan sediments provided strong support for the use of biomarkers to trace C source in fjords despite conflicting elemental and isotopic bulk sediment signature. However, whether net plant storage increases or decreases cannot be resolved without resolving disagreements between the bulk sediment elemental and isotopic data and characterizing degradation in these environments. Due to the outsized capacity for atmospheric CO_2 sequestration of vascular plants, the absolute and relative increase of terrestrial plant wax biomolecules preserved in increasingly deglaciated and vegetated fjord sediments suggests deglaciated mid-latitude fjords may act as a carbon sink as global temperatures continue to rise.

Acknowledgements

A special thanks to Dr. Maureen Walczak, Dr. Randie Bundy, Dr. Camilo Ponton and my entire mentorship team for their patient guidance and skilled expertise. This research was made possible by the incredible School of Oceanography faculty and the many impromptu helpers who helped a stranger push her science forward.

References

Black, T., & Kurtz, D. (2023). Maritime glacier retreat and terminus area change in Kenai Fjords National Park, Alaska, between 1984 and 2021. *Journal of Glaciology*, *69*(274), 251–265. https://doi.org/10.1017/jog.2022.55

Bush, R. T., & McInerney, F. A. (2013). Leaf wax n-alkane distributions in and across modern plants: Implications for paleoecology and chemotaxonomy. *Geochimica et Cosmochimica Acta*, *117*, 161–179. https://doi.org/10.1016/j.gca.2013.04.016

Chevalier, N., Savoye, N., Dubois, S., Lama, M. L., David, V., Lecroart, P., et al. (2015). Precise indices based on n-alkane distribution for quantifying sources of sedimentary organic matter in coastal systems. *Organic Geochemistry*, *88*, 69–77. https://doi.org/10.1016/j.orggeochem.2015.07.006

Ciais, P., Tagliabue, A., Cuntz, M., Bopp, L., & Et., A. (2011). Large inert carbon pool in the terrestrial biosphere during the Last Glacial Maximum. *Nature Geoscience*. https://doi.org/10.1038/ngeo1324

Cosma, T., & Hendy, I. L. (2008). Pleistocene glacimarine sedimentation on the continental slope off Vancouver Island, British Columbia. *Marine Geology*, *255*(1–2), 45–54. https://doi.org/10.1016/j.margeo.2008.07.001

Crowley, T. J. (1995). Ice Age terrestrial carbon changes revisited. *Global Biogeochemical Cycles*, *9*(3), 377–389. https://doi.org/10.1029/95GB01107

Cui, X., Bianchi, T. S., Jaeger, J. M., & Smith, R. W. (2016). Biospheric and petrogenic organic carbon flux along southeast Alaska. *Earth and Planetary Science Letters*, *452*, 238–246. https://doi.org/10.1016/j.epsl.2016.08.002

Davies, Mix, A. C., Stoner, J. S., Addison, J. A., Jaeger, J., Finney, B., & Wiest, J. (2011). The deglacial transition on the southeastern Alaska Margin: Meltwater input, sea level rise,

marine productivity, and sedimentary anoxia. *Paleoceanography*, *26*(2), 2010PA002051. https://doi.org/10.1029/2010PA002051

Davies, B., Bendle, J., Carrivick, J., McNabb, R., McNeil, C., Pelto, M., et al. (2022). Topographic controls on ice flow and recession for Juneau Icefield (Alaska/British Columbia). *Earth Surface Processes and Landforms*, *47*(9), 2357–2390. https://doi.org/10.1002/esp.5383

Davies, B., McNabb, R., Bendle, J., Carrivick, J., Ely, J., Holt, T., et al. (2024). Accelerating glacier volume loss on Juneau Icefield driven by hypsometry and melt-accelerating feedbacks. *Nature Communications*, *15*, 5099. https://doi.org/10.1038/s41467-024-49269-y

Eglinton and Hamilton. (1967). Leaf Epicuticular Waxes.

Friedlingstein, P., O'Sullivan, M., Jones, M. W., Andrew, R. M., Hauck, J., Landschützer, P., et al. (2025). Global Carbon Budget 2024. *Earth System Science Data*, *17*(3), 965–1039. https://doi.org/10.5194/essd-17-965-2025

Goranov, A. I., Carter, S. J., Pearson, A., & Hatcher, P. G. (2025). Oxidation Camouflages Terrestrial Organic Matter to Appear Marine-like. *Environmental Science & Technology*, *59*(11), 5607–5620. https://doi.org/10.1021/acs.est.4c12913

Harris, A. S., Hutchison, K., Meehan, W. R., Swanston, D. N., Helmers, A. E., Hendee, J. C., & Collins, T. M. (1974). THE FOREST ECOSYSTEM OF SOUTHEAST ALASKA I.The Setting.

Heaton, T. J., Köhler, P., Butzin, M., Bard, E., Reimer, R. W., Austin, W. E. N., et al. (2020). Marine20—The Marine Radiocarbon Age Calibration Curve (0–55,000 cal BP). *Radiocarbon*, *62*(4), 779–820. https://doi.org/10.1017/RDC.2020.68

Hedges. (1992). Global biogeochemical cycles: progress and problems. *Marine Chemistry*, *39*(1), 67–93. https://doi.org/10.1016/0304-4203(92)90096-S

Hedges, & Keil, R. G. (1995). Sedimentary organic matter preservation: an assessment and speculative synthesis. *Marine Chemistry*, *49*(2–3), 81–115. https://doi.org/10.1016/0304-4203(95)00008-F

Hedges, & Oades, J. M. (1997). Comparative organic geochemistries of soils and marine sediments. *Organic Geochemistry*, *27*(7–8), 319–361. https://doi.org/10.1016/S0146-6380(97)00056-9

Horn, A. T. (2021, September 3). Sample Weight Calculator | Stable Isotope Facility. Retrieved June 4, 2026, from https://stableisotopefacility.ucdavis.edu/sample-weight-calculator

Jaeger, Gulick, S. P. S., & LeVay, L. J. (2014). Site U1417. In *Proceedings of the Integrated Ocean Drilling Program, Volume 341: Expedition Reports Southern Alaska Margin* (Vol. 341). https://doi.org/10.2204/iodp.proc.341.103.2014

Jaeger, J. M., & Koppes, M. N. (2016). The role of the cryosphere in source-to-sink systems. *Earth-Science Reviews*, *153*, 43–76. https://doi.org/10.1016/j.earscirev.2015.09.011

Jaeger, J. M., & Nittrouer, C. A. (2006). A quantitative examination of modern sedimentary lithofacies formation on the glacially influenced Gulf of Alaska continental shelf. *Continental Shelf Research*, *26*(17–18), 2178–2204. https://doi.org/10.1016/j.csr.2006.07.014

Jeltsch-Thömmes, A., Battaglia, G., Cartapanis, O., Jaccard, S. L., & Joos, F. (2019). Low terrestrial carbon storage at the Last Glacial Maximum: constraints from multi-proxy data. *Climate of the Past*, *15*(2), 849–879. https://doi.org/10.5194/cp-15-849-2019

Key, R. M., Kozyr, A., Sabine, C. L., Lee, K., Wanninkhof, R., Bullister, J. L., et al. (2004). A global ocean carbon climatology: Results from Global Data Analysis Project (GLODAP). *Global Biogeochemical Cycles*, *18*(4), 2004GB002247. https://doi.org/10.1029/2004GB002247

Kim, J.-H., Peterse, F., Willmott, V., Kristensen, D. K., Baas, M., Schouten, S., & Sinninghe Damsté, J. S. (2011a). Large ancient organic matter contributions to Arctic marine

sediments (Svalbard). *Limnology and Oceanography*, *56*(4), 1463–1474. https://doi.org/10.4319/lo.2011.56.4.1463

Kim, J.-H., Peterse, F., Willmott, V., Kristensen, D. K., Baas, M., Schouten, S., & Sinninghe Damsté, J. S. (2011b). Large ancient organic matter contributions to Arctic marine sediments (Svalbard). *Limnology and Oceanography*, *56*(4), 1463–1474. https://doi.org/10.4319/lo.2011.56.4.1463

Kolattukudy, P. (2001). Plant Cuticle and Suberin. In Wiley, *Encyclopedia of Life Sciences* (1st ed.). Wiley. https://doi.org/10.1038/npg.els.0001920

Maslin, M. A., & Swann, G. E. A. (2006). ISOTOPES IN MARINE SEDIMENTS. In M. J. Leng (Ed.), *Isotopes in Palaeoenvironmental Research* (Vol. 10, pp. 227–290). Dordrecht: Springer Netherlands. https://doi.org/10.1007/1-4020-2504-1_06

Meyers, P. A., Bourbonniere, R. A., & Takeuchi, N. (1980). Hydrocarbons and fatty acids in two cores of Lake Huron sediments. *Geochimica et Cosmochimica Acta*, *44*(8), 1215–1221. https://doi.org/10.1016/0016-7037(80)90075-7

Nuwer, J. M., & Keil, R. G. (2005). Sedimentary organic matter geochemistry of Clayoquot Sound, Vancouver Island, British Columbia. *Limnology and Oceanography*, *50*(4), 1119–1128. https://doi.org/10.4319/lo.2005.50.4.1119

Sigman, D. M., & Boyle, E. A. (2000). Glacial/interglacial variations in atmospheric carbon dioxide. *Nature*, *407*(6806), 859–869. https://doi.org/10.1038/35038000

Smith, R. W., Bianchi, T. S., Allison, M., Savage, C., & Galy, V. (2015). High rates of organic carbon burial in fjord sediments globally. *Nature Geoscience*, *8*(6), 450–453. https://doi.org/10.1038/ngeo2421

Syvitski, J. P. M., Burrell, D. C., & Skei, J. M. (1987). *Fjords: Processes and Products*. New York, NY: Springer New York. https://doi.org/10.1007/978-1-4612-4632-9

Walczak, M. H., Mix, A. C., Cowan, E. A., Fallon, S., Fifield, L. K., Alder, J. R., et al. (2020). Phasing of millennial-scale climate variability in the Pacific and Atlantic Oceans. *Science*, *370*(6517), 716–720. https://doi.org/10.1126/science.aba7096

Walinsky, S. E., Prahl, F. G., Mix, A. C., Finney, B. P., Jaeger, J. M., & Rosen, G. P. (2009). Distribution and composition of organic matter in surface sediments of coastal Southeast Alaska. *Continental Shelf Research*, *29*(13), 1565–1579. https://doi.org/10.1016/j.csr.2009.04.006

Wang, N., Zong, Y., Brodie, C. R., & Zheng, Z. (2014). An examination of the fidelity of n-alkanes as a palaeoclimate proxy from sediments of Palaeolake Tianyang, South China. *Quaternary International*, *333*, 100–109. https://doi.org/10.1016/j.quaint.2014.01.044

Zeng, N. (2003). Glacial-interglacial atmospheric CO2 change —The glacial burial hypothesis. *Advances in Atmospheric Sciences*, *20*(5), 677–693. https://doi.org/10.1007/BF02915395

Zhang, J., & Gulick, S. P. S. (2020). Sequence stratigraphy and depositional history of the Baranof Fan: Insights for Cordilleran Ice Sheet outflow to the Gulf of Alaska. *GSA Bulletin*, *132*(1–2), 353–372. https://doi.org/10.1130/B35164.1

Zonneveld, K. A. F., Versteegh, G. J. M., Kasten, S., Eglinton, T. I., Emeis, K.-C., Huguet, C., et al. (2009, July 1). Selective preservation of organic matter in marine environments – processes and impact on the fossil record. Biogeochemistry: Organic Biogeochemistry. https://doi.org/10.5194/bgd-6-6371-2009

Zurbuchen, J. M., Gulick, S. P. S., Walton, M. A. L., & Goff, J. A. (2015). Imaging evidence for Hubbard Glacier advances and retreats since the last glacial maximum in Yakutat and Disenchantment Bays, Alaska. *Geochemistry, Geophysics, Geosystems*, *16*(6), 1962–1974. https://doi.org/10.1002/2015GC005815